DEVELOPMENT OF A COMPRESSION-ABSORPTION HEAT PUMP SYSTEM FOR UTILIZING LOW TEMPERATURE GEOTHERMAL WATER

by

Yulie GONG[a,b,c], Chao LUO[a,b,c,d*], Zhenneng LU[a,b,c], Yuan YAO[a,b,c], and Weibin MA[a,b,c]

[a]Guangzhou Institute of Energy Conversion, Chinese Academy of Sciences, Guangzhou, Guangdong, China
[b]Key Laboratory of Renewable Energy, Chinese Academy of Sciences, Guangzhou, Guangdong, China
[c]Guangdong Provincial Key Laboratory of New and Renewable Energy Research and Development, Guangzhou, Guangdong, China
[d]Key Laboratory of Efficient Utilization of Low and Medium Grade Energy (Tianjin University), Ministry of Education, Tianjin, China

Original scientific paper
https://doi.org/10.2298/TSCI170826241G

Heat pump is an effective way to use the low temperature geothermal water with temperature lower than 50 ℃ for building heating. Compared to the conventional vapour compression heat pump, the compression-absorption heat pump (CAHP) can obtain higher heat sink temperature with lower compression ratio. Besides, the temperature glide in the generator and absorber of CAHP can be fitted to the heat source and heat sink, which achieves better coefficient of performance. Two models, respectively, for the generator and whole system using ammonia-water (NH_3-water) as the working fluid are proposed, and the effects of different concentration of strong solution, cycle ratios, heat source temperature and spray density on the generator are investigated. The objective is to analyse the performance of CAHP system driven by low temperature geothermal water. The results show that the maximum of overall heat transfer coefficient of the vertical out-tube falling film generator can be obtained with the optimum spray density of around 0.16 kg/ms and there is an optimum concentration of around 65% for the CAHP system. When the low heat source temperature between 30 ℃ and 40 ℃, the high heat sink temperature can reach to 65-70 ℃.

Key words: *geothermal water, CAHP, vertical out-tube falling film, generator, NH_3-water*

Introduction

With the drastic increase of fossil energy consumption for residents heating, the environment deteriorated rapidly all around the world. Because of the renewable capacity and cleanness, geothermal energy is one of the most promising renewable energy resources [1-4]. In China, a large amount of geothermal energy lower than 50 ℃ in the form of low-grade energy cannot be used for residents heating due to difficulties of transforming the energy into useful high-grade energy. Heat pump is an efficient way to upgrade low temperature geothermal water up to a more feasible high temperature for residents heating and reduce the fossil

* Corresponding author, e-mail: luochao@ms.giec.ac.cn

energy consumption and CO_2 emission [5-7]. Compared to conventional vapour compression heat pumps, the CAHP cycle provides a number of attractive advantages [8, 9]. The CAHP can obtain a higher heat sink temperature with a lower compression ratio [10, 11] and the generator and absorber temperature glide can be fitted to gliding temperatures of the heat source and heat sink, which leading to a higher COP. Besides, the CAHP can be operated efficiently with low-temperature water [12].

The heat transfer coefficient of the generator has great influence on COP of the CAHP. Rameshkumar *et al*. [13, 14] studied a heat transfer model of aqua ammonia GAXAC system and the results showed that the COP increased sharply as heat transfer in the generator increased. Absorption/compression cycles were carried out in 1950 and research activities have increased rapidly since 1980, the design of the heat exchangers and compressors, and the choice of working fluids are evaluated [15]. Chun and Seban [16] conducted falling film generation heat transfer experiments of water on the outside surface of vertical tube and published important experimental data. So far, the experimental data have been used by many investigators to validate the theoretical simulations of falling film heat transfer. Compression heat pump with solution circuit (CHSC) has two major advantages: the heating capacity is easily varied by a large factor by adjusting the composition of the mixture and the approximation of the Lorenz process allows for substantially high COP values in cases with gliding temperatures [17]. The area distributed to the solution heat exchanger (SHE) and the concentration of NH_3-water have impact on COP of CAHP, and the falling-film tubes should be designed to be as long as possible in order to increase the COP [18, 19]. But the application of vertical falling-film heat exchangers in CAHP generator is still very infrequent. So, it is necessary to develop a new simulation model to optimize heat transfer of the vertical falling-film generator. The advantages of vertical falling-film heat transfer are widely recognized, but as for the low temperature heat source is very limited.

In this paper, a CAHP system applied vertical falling-film generator to utilize low temperature geothermal water for building heating is developed. Models for the vertical out-tube falling film generator and the whole system using NH_3-water as the working fluid are established. With respect to working fluids, the NH_3-water mixture is the most interesting one because of its excellent properties and large experience handling in industrial applications. The performance of CAHP system driven by low temperature geothermal water is analysed and effects of different concentration of strong solution, heat source temperature and spray density on the generator are investigated. Comparing with the traditional compression heat pump, CAHP can get a high heat sink temperature with a lower compression ratio, and the system can be operated efficiently with low temperature water.

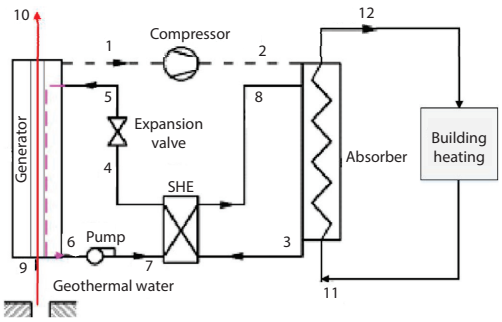

Figure 1. Schematic diagram of CAHP system; *1 – low pressure ammonia vapour, 2 – high pressure ammonia vapour, 3 – rich solution with low temperature, 4 – rich solution with high temperature, 5 – rich solution with low pressure, 6 – weak solution with low pressure, 7 – weak solution with high pressure, 8 – weak solution with low temperature, 9 – geothermal water inlet, 10 – geothermal water outlet, 11 – building heating water in absorber, 12 – building heating water out of absorber*

System description

A CAHP cycle includes a vertical falling-film generator, a pump, a SHE, an absorber, a reducing valve and a compressor, as shown in fig. 1. According to former studie [15], the

NH_3-water mixture is chosen as the working pair for the CAHP. The compressor increases the pressure of ammonia desorbed from the generator to a high level and then the ammonia enter the absorber. In the absorber, the ammonia gases are absorbed by the weak solution while the absorption heat is released to the heat sink. After that the rich solution preheats the weak solution in the SHE and passes through the expansion valve and then enters the generator again.

Model establishment

Generator model

The schematic of the generator is represented in fig. 2. The generator is a single-pass counter current vertical out-tube falling film heat exchanger with the solution outside the smooth tubes and the geothermal water inside the tubes. Take the liquid film flow direction as *x*-direction and vertical direction as *y*-direction. The following assumptions are made to simplify the mathematical model:

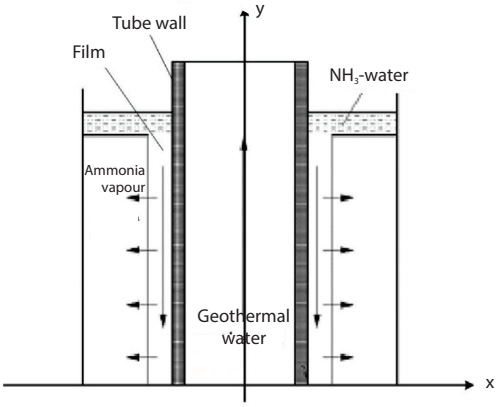

Figure 2. Schematic diagram of a vertical out-tube falling film generator

- heat transfer by conductivity in the direction of flow is negligible,
- the fluid outside the tube is regarded as Newtonian fluid and flow is unsteady,
- mass transfer resistance is negligible,
- fluid is ideally mixed in the direction perpendicular to the flow,
- there is no interaction force between the liquid and vapour, and
- there is no heat transfer between the liquid and vapour except evaporation heat.

The governing equations are given:

- continuity equation:

$$\frac{\partial(\rho U)}{\partial x}+\frac{\partial(\rho V)}{\partial y}=0 \tag{1}$$

- momentum equation:

$$\rho U\frac{\partial U}{\partial x}+\rho V\frac{\partial U}{\partial y}=\frac{\partial}{\partial y}\left(\mu\frac{\partial U}{\partial y}\right)+\rho g \tag{2}$$

- energy equation:

$$\rho C_P U\frac{\partial T}{\partial x}+\rho C_P V\frac{\partial T}{\partial y}=\frac{\partial}{\partial y}\left(\lambda\frac{\partial T}{\partial y}\right) \tag{3}$$

- mass conservation equation:

$$\rho U\frac{\partial \xi}{\partial x}+\rho V\frac{\partial \xi}{\partial y}=\frac{\partial}{\partial y}\left(\rho D_m\frac{\partial \xi}{\partial y}\right) \tag{4}$$

The boundary conditions are given:

- entrance boundary conditions:

$$\delta\big|_{x=0}=\delta_0 \tag{5}$$

$$V\big|_{x=0}=0 \tag{6}$$

$$T\big|_{x=0}=0 \tag{7}$$

$$\xi\big|_{x=0}=\xi_0 \tag{8}$$

$$U\Big|_{x=0}=\frac{\Gamma}{\rho\delta_0}\big|x=0 \tag{9}$$

– no slip boundary condition:

$$U\Big|_{y=0}=V\Big|_{y=0} \tag{10}$$

– non-filtration boundary conditions:

$$\frac{\partial\xi}{\partial y}\Big|_{y=0}=0 \tag{11}$$

$$T\big|_{y=0}=T_0 \tag{12}$$

– boundary conditions of liquid-vapour interface:

$$\lambda\frac{\partial T}{\partial y}\Big|_{y=\delta}=-\Delta H\frac{\rho D_m}{\xi}\frac{\partial\xi}{\partial y} \tag{13}$$

$$\frac{\partial U}{\partial y}\Big|_{y=0}=0 \tag{14}$$

$$F(p_g,T_f,C_f)\big|_{y=0}=0 \tag{15}$$

Table 1. Inputs of the generator model

Variable	Value	Variable	Value
δ	2 mm	V_w	0.1-0.5 [m^{3}h^{-1}]
H	5 m	p	0.2-2 [MPa]
D_i	21 mm	v	0
D_o	25 mm	Γ	0.06-0.26 [kgm^{-1}s^{-1}]
ξ	55-70%	T_9	30-40 [°C]

$$\dot{m}\Big|_{y=\delta}=\left(-\rho V+\rho U\frac{\mathrm{d}\delta}{\mathrm{d}x}\right)\Big|_{y=\delta}=-\frac{\rho D_m}{\xi}\frac{\partial\xi}{\partial y}_{|y=\delta} \tag{16}$$

The flow rate, solution concentration and temperature can be calculated by the previous mathematical model and the input parameters of the generator model are shown in tab. 1.

System model

The system analysis is carried out for heating applications with the following assumptions:

– the system is working under steady-state conditions,
– the processes in absorber and generator are considered adiabatic, and the process in the expansion valve is isenthalpic,
– the weak solution at the exit of the generator and the strong solution at the exit of absorber are saturated,
– the effect of pressure drops in various components on the system performance are assumed to be negligible, and
– due to the large difference between the boiling points of water and ammonia, the concentration of the vapour is considered as 99.8%.

The correlations proposed by Xu [20] are used to calculate the thermodynamic properties of the saturated solution and vapour. Chemical equilibrium is assumed at the exit of each component. The energy balance across the components is showed:

– generator:

$$Q_{gw} + \dot{m}_5 h_5 = \dot{m}_6 h_6 + \dot{m}_1 h_1 \tag{17}$$

$$Q_{gw} = \dot{m}_{gw}(h_9 - h_{10}) = \dot{m}_{gw} k_g A_g \Delta T_g \tag{18}$$

$$\dot{m}_6 + \dot{m}_1 = \dot{m}_5 \tag{19}$$

– compressor:

$$W_c = \frac{\dot{m}_1(h_2 - h_1)}{\eta_{is}} \tag{20}$$

– absorber:

$$Q_a + \dot{m}_3 h_3 = \dot{m}_8 h_8 + \dot{m}_1 h_2 \tag{21}$$

$$\dot{m}_3 = \dot{m}_8 + \dot{m}_1 \tag{22}$$

$$Q_a + \dot{m}_{aw}(h_{12} - h_{11}) = \dot{m}_{aw} k_a A_a \Delta T_a \tag{23}$$

– pump:

$$W_p = \frac{\dot{m}_6(h_1 - h_6)}{\eta_p} \tag{24}$$

– compression ratio:

$$\varepsilon = \frac{p_2}{p_1} \tag{25}$$

At each pressure ratio, according to a screw compressor cooled with an insoluble oil, the isentropic efficiency data used [18, 19]:

$$\eta_{is} = -0.143 + 0.55\varepsilon - 0.0867\varepsilon \quad \text{for} \quad \varepsilon = 2 \sim 3.5 \tag{26}$$

$$\eta_{is} = -0.766 + 0.0131\varepsilon \quad \text{for} \quad \varepsilon = 3.5 \sim 10 \tag{27}$$

$$\text{COP} = \frac{Q_a}{W_c + W_p} \tag{28}$$

Results and discussion

Figure 3 illustrates the effect of the value of the inlet spray density, Γ, on the overall heat transfer coefficient, U_g, of the generator. When the water temperature, T_9, and volume flow, V_g, are kept constant at 30 °C and 0.5 m^3/h, respectively, the U_g firstly increases and then decreases with the increasing Γ. This phenomenon can be explained from the fact that larger spray density bring higher velocity of film flow and high velocity will be beneficial to improve the heat transfer of generator. However, the film will became thicker if spray density exceeds the optimum value and results in the decrease of the heat transfer efficiency. Figure 4 shows that when the heat source temperature increases, the U_g increases linearly. Under the same condition, when the temperature is blow 40 °C, the difference of U_g at different spray densities is small. According to figs. 3 and 4, the spray density and the geothermal temperature have positive effects on heat transfer of generator which is benefit to the system performance and the optimum value of spray density is around 0.16 kg/ms.

Figure 5 shows the cycle ratio changes along with spray densities. It can be seen from fig. 5 that the cycle ratio increases with spray density increasing and it increases slowly when the Γ is in the range from 0.06 kg/ms to 0.2 kg/ms. It can be seen from fig. 6 that the heat source temperature has significant impact on the concentration difference and cycle ratio. In the CAHP

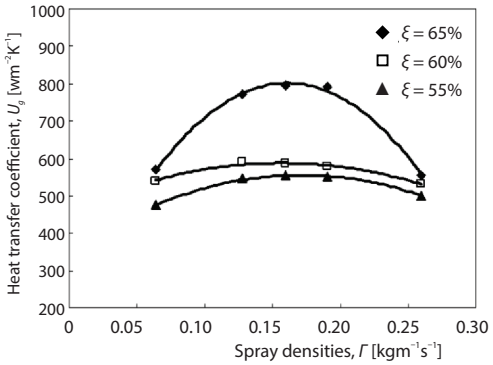

Figure 3. The U_g-Γ relation with different strong solution concentration (geothermal water temperature T_9 = 30 °C, volume flow rate V_g = 0.5 m^3/h)

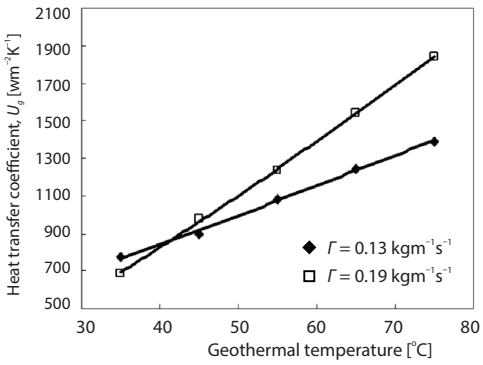

Figure 4. The changes of U_g along with geothermal water temperature at different spray densities (geothermal water V_g = 0.5 m^3/h, strong solution concentration ξ = 65%)

system the cycle ratio has a large effect on COP [13, 14], which means the spray densities and the heat source temperature also makes a different influence on COP. When the concentration is 65%, a high concentration difference about 10% can be obtained.

Figure 7 shows that for different geothermal water inlet temperatures, T_9, compression ratio, ε, decreasing as the concentration increases. The changes of concentration have great influence on the compression ratio. The COP changes along with the variation of T_9 shown in fig. 8. Each curve shows the COP as a function of concentration, and at the same concentration, COP is larger for higher heat source temperature. All of those curves shows that when the concentration is larger than 65%, the COP of the system is almost constant. That is because the heat of dissolution for unit mass of ammonia in different conditions is subequal. If the compression ratio increases, indicating that the work input to the compressor becomes lager, the system COP decreased. It is worthy to note that as the heat sink temperature is 65 °C and the heat source temperature is higher than 30 °C, the COP is always higher than 4.0.

The dependence of compression ratio on heat sink temperature, T_{12}, for different values of concentration is shown in fig. 9. The lower the concentration causes the higher the compression ratio, which means more power input is needed for the system. The COP changes

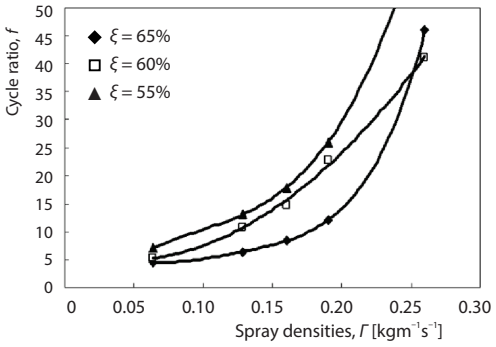

Figure 5. The f-Γ relation with different strong solution concentration (geothermal water temperature T_9 = 30 °C, volume flow rate V_g = 0.5 m^3/h)

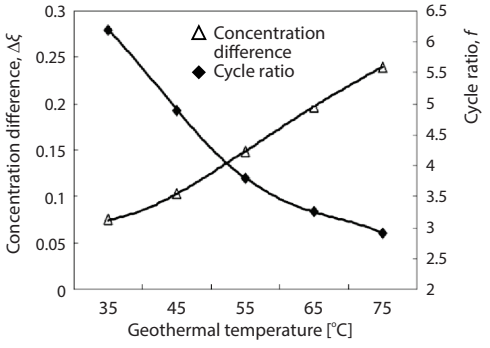

Figure 6. The effect of geothermal water temperature on concentration difference and cycle ratio (spray density Γ = 0.13 kg/ms, geothermal water V_g = 0.5 m^3/h, strong solution concentration ξ = 65%)

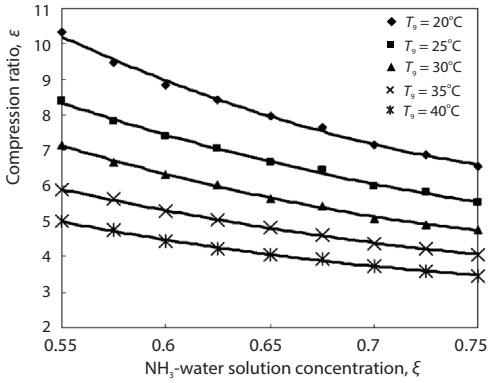

Figure 7. The changes of ε along with concentration at different heat source temperatures (heat sink temperature T_{12} = 65 °C)

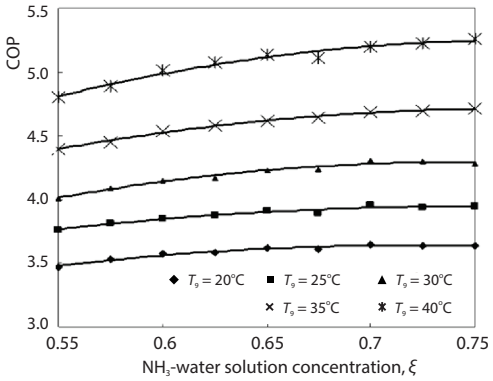

Figure 8. The changes of COP along with concentration at different heat source temperatures (heat sink temperature T_{12} = 65 °C)

along with the heat sink temperature, T_{12}, shown in fig. 10. The COP changes sharply with the heat sink temperature and higher concentration can get higher COP, but the influence is diminishing with the increase of concentration. When the concentration is greater than 70%, the COP almost does not change with the concentration, indicating that there should be an optimal concentration value for this system. According to the previous analysis, the optimal value of solution concentration is around 65%.

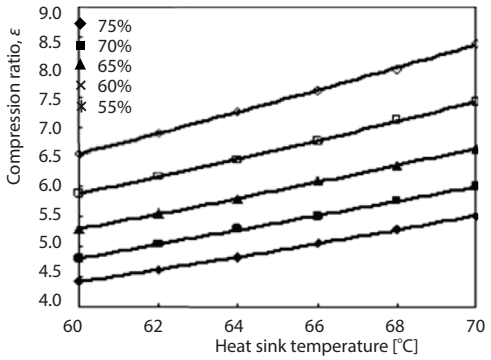

Figure 9. The changes of ε along with heat sink temperature at different concentrations (heat source temperature T_9 = 30 °C)

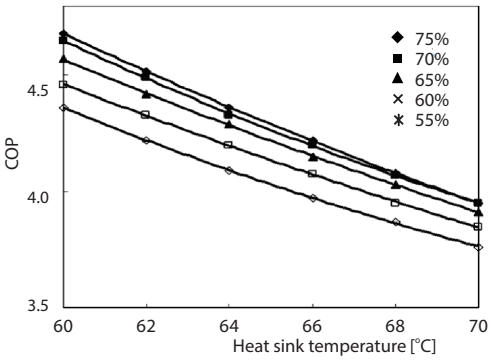

Figure 10. The changes of COP along with heat sink temperature at different concentrations (heat source temperature T_9 = 30 °C)

Conclusions

A specialized numerical model for the generator and a model for the CAHP system using low temperature geothermal water have been studied. The following conclusions can be drawn.

- The model indicates that the CAHP system is appropriate for utilizing low temperature geothermal water, when the system operating with a high heat sink temperature between 65 °C and 75 °C and a low heat source temperature from 30-40 °C.
- The spray density, the concentration and heat source temperature have the great effects on the performance of the generator at the low temperature condition. The maximum over all

heat transfer coefficient of the out-tube falling film generator can be obtained in an optimum spray density of around 0.16 kg/ms. When the concentration is 65%, it can get a high concentration difference about 10%.

- The COP increases with the concentration increases. There also exists an optimum concentration value of around 65%.

Acknowledgment

The research work has been financially supported by the Guangdong province science and technology project (No.2013B091500087), National Natural Science Funds (51406212) and the Science and Technology Plan Projects of Guangdong Province (2017A030223009).

Nomenclature

A – heat transfer area, [mm]
A_a – area of absorber, [m^2]
A_g – area of generator, [m^2]
D_i – inner diameter, [mm]
D_m – mass transfer coefficient, [ms^{-1}]
D_0 – outside diameter, [mm]
f – cycle ratio, [–]
H – generator height, [m]
h – enthalpy, [kJkg^{-1}]
K_a – specific heat at sonstant pressure of absorber, [kJkg^{-1}K^{-1}]
K_g – specific heat at sonstant pressure of generator, [kJkg^{-1}K^{-1}]
k – overall heat transfer koefficient, [Wm^{-2}K^{-1}]
$\dot{m}$ – mass-flow, [kgs^{-1}]
p – pressure, [MPa]
Q_a – heat capacity of generator [kW]
Q_{gw} – heat capacity of generator [kW]
T – temperature, [K]
U_g – heat transfer coefficient of generator, [Wm^{-2}K^{-1}]
V – volume flow, [m^{3}h^{-1}]
u, v – velocity of y-direction, [ms^{-1}]
W_c – power imput of compressor [kW]
W_p – power imput of pump [kW]

Greek symbols

Γ – inlet spray density, [kgm^{-1}s^{-1}]
δ – film thickness, [mm]
ε – compression ratio, [–]
λ – coefficient of heat conductivity, [Wm^{-1}K^{-1}]
η_{is} – isentropic efficiency, [–]
η_p – efficiency of the pump, [–]
ξ – solution concentration, [%]
ρ – density, [kgm^{-3}]

Subscripts

1~12 – condition points of fig. 1
0 – initial state
a – absorber
g – generator
w – water

References

[1] Edouard, W., *et al.*, Heat Recovery in Compost Piles for Building Applications, *Thermal Science*, *21* (2017), 2, pp. 775-784
[2] Stojković, J. S., *et al.*, The Analysis of the Geothermal Energy Capacity for Power Generation in Serbia, *Thermal Science*, *17* (2013), 4, pp. 969-976
[3] Urbancl, D., *et al.*, Geothermal Heat Potential – The Source for Heating Greenhouses in Southestern Europe, *Thermal Science*, *20* (2016), 4, pp. 1061-1071
[4] Borsukiewicz-Gozdur, A., Nowak, W., Feasibility Study and Energy Efficiency Estimation of Geothermal Power Station Based on Medium Enthalpy Water, *Thermal Science*, *11* (2007), 3, pp.135-142
[5] Milovančević, U. M., Kosi, F. F., Performance Analysis of System Heat Pump – Heat Recuperator Used for Air Treatment in Process Industry, *Thermal Science*, *20* (2016), 4, pp.1345-1354
[6] Li, M. Y., Lior, N., Analysis of Hydraulic Fracturing and Reservoir Performance in Enhanced Geothermal Systems, *Journal of Energy Resources Technology – Transactions of the ASME*, *137* (2015), 4, 041203
[7] Wong, K. V., Sustainable Engineering in the Global Energy Sector, *Journal of Energy Resources Technology*, *138* (2015), 4, 024701
[8] Bourouis, M., *et al.*, Industrial Heat Recovery by Absorption/Compression Heat Pump Using TFE-H_2O-TEGDME Working Mixture, *Applied Thermal Engineering*, *20* (2000), 4, pp. 355-369
[9] Selahattin, G., Ismail D., The Optimum Performance of a Solar-Assisted Combined Absorption – Vapor Compression System for Air Conditioning and Space Heating, *Solar Energy*, *71* (2001), 3, pp. 213-216

[10] Ahlby, L., *et al.*, Optimization Study of the Compression/Absorption Cooling Cycle, *International Journal of Refrigeration*, *14* (1991), 1, pp. 16-23
[11] Brunin, O., *et al.*, Compression of the Working Domains of Some Compression Heat Pumps and a Compression-Absorption Heat Pump, *International Journal of Refrigeration*, *20* (1997), 5, pp. 308-318
[12] Fukuta, M., *et al.*, Performance of Compression/Absorption Hybrid Refrigeration Cycle with Propane/Mineral Oil Combination, *International Journal of Refrigeration*, *25* (2002), 7, pp. 907-915
[13] Rameshkumar, A., *et al.*, Heat Transfer Studies on a GAXAC (Generator-Absorber-Exchange Absorption Compression) Cooler, *Applied Energy*, *86* (2009), 10, pp. 2056-2064
[14] Rameshkumar, A., *et al.*, Energy Analysis of a 1-Ton Generator-Absorber-Exchange Absorption-Compression (GAXAC) Cooler, *ASHRAE Transactions*, *115* (2009), 1, pp. 405-414
[15] Groll, E.A., Current Status of Absorption/Compression Cycle Technology, ASHRAE Transactions, *Technical and symposium papers*, *103* (1997), 1, p. 1136
[16] Chun, K. R., Seban, R. A., Heat Transfer to Evaporating Liquid Film, A*SME J. Heat Transfer*, *93* (1971), 3, pp. 391-396
[17] Stokar, M., Trepp, C., Compression Heat Pump with Solution Circuit – Part 1: Design and Experimental Results, *International Journal of Refrigeration*, *10* (1986), 2, pp. 87-96
[18] Hulten, M., Berntsson, T., The Compression/Absorption Heat Pump Cycle-Conceptual Design Improvements and Comparison with the Compression Cycle, *International Journal of Refrigeration*, *25* (2002), 4, pp. 487-497
[19] Hulten, M., Berntsson, T., The Compression/Absorption Cycle-Influence of Same Major Parameters on COP and a Comparison with the Compression Cycle, *International Journal of Refrigeration*, *22* (1999), 2, pp. 91-106
[20] Xu, S. M., Derivation of NH_3-H_2O Thermodynamic Parameters Expression and Programming (in Chinese), *Fluid Machinery*, *23* (1995), 2, pp.55-59

Paper submitted: August 26, 2017
Paper revised: November 9, 2017
Paper accepted: November 13, 2017